JOURNAL OF THE KOREAN ASTRONOMICAL SOCIETY
31: 77 ~ 87, 1998

A SIMPLE GRANULE MODEL AND ITS EFFECT ON SPECTRAL LINE ASYMMETRY

KIM, YONGCHEOL
Center for Space Astrophysics Yonsei University Seoul, Korea
kim@csa.yonsei.ac.kr
(Received Apr. 29, 1998; Accepted Aug. 10,1998)

ABSTRACT

The accumulated knowledge of the influence of *solar* granulation on spectral lines, i.e. their asymmetry, provides a key to analyze *stellar* spectral line asymmetries. In this paper, a simple line synthesis using a simple 'model' of granulation was calculated. By adjusting the properties of the granule model, the observed imprints of convection on spectral lines can be reproduced. Since we depict convective flows using a continuous function rather than using a few components of flows (*cf.*Gray and Toner 1985, 1986; dravins 1990), we were able to identify which components of convection are important in line bisector shapes.
The results of this study can be summarized as follows: Firstly, the intensity contrast (i.e. temperature fluctuation), and the area coverage of up- and down-flows are the two important factors which determine the line bisector shapes. Secondly, on the contrary to the assumption of other studies, the effect of horizontal flows is non-negligible. This exercise provides a qualitative understanding of the effect of convection on spectral lines. This knowledge serves as a guideline for understanding the characteristic difference in convection for stars on either side of the "Granulation Boundary" (Gray 1982; Gray and Nagel 1989).

Key Words : Convection, Spectral line profiles

I. INTRODUCTION

(a) Solar Spectral Line Asymmetries

It has been known for a century that the wavelengths of solar spectral lines are not identical to those of lines in laboratory comparison sources Jewell 1896). After corrections for the Sun-Earth motion and gravitational redshift, a typical photospheric line has seemed to show a blueshift of 300 $\sim$ 400 $m\ sec^{-1}$ (Pierce and Breckinridge 1973). Halm (1907) discovered that the wavelength discrepancy changes across the solar disk. Considering that the maximum accuracies in laboratory wavelengths were on the order of 100 $m\ sec^{-1}$, Higgs (1960, 1962) emphasized that solar photospheric spectral lines are not symmetric at that level of accuracy. Higgs stressed the uncertainty in the wavelength determinations of solar spectral lines, which originated from the line profile asymmetries. Since then, the line asymmetry has been measured and studied extensively (e.g. Magnan and Pecker 1974, Gurtovenko *et al.* 1975).

To explain solar line wavelength shifts (in other words, line asymmetries), many mechanisms have been suggested. Melnikov (1964) and Magnan and Pecker (1974) reviewed these various theories. It has been concluded that convection causes the observed line asymmetry (kostik *et al.* 1977b).

(b) Line Bisectors

A line bisector is a widely used indicator of the line profile asymmetry. It is defined as the locus of the midpoints of line segments which connect equal-intensity points on either wing of a line profile, as shown in figure 1. Therefore, the bisector divides the absorption line into two halves of equal equivalent width, and shows the apparent radial velocity at each depth in the line. Different parts of a stellar spectral line profile are produced at different depths of the atmosphere. Line cores are formed in the upper level of the atmosphere, while wings are produced further down. As a result, the shift and curvature at each point along a bisector can provide information of condition at different depths of stellar atmosphere.

The line bisector was introduced in solar studies by Voigt (1956, 1957), and was later used for a quantitative analysis of large scale solar motions by De Jager and Neven (1967), who showed that it reflects the effects of convection in the solar atmosphere. Using line bisectors, Kostik and Orlova (1970, 1977a, 1977b) extensively studied the asymmetry of solar lines of different strength and different center to limb positions. The temporal as well as the spatial change in bisector shapes was observed by Gurtovenko (1972).

Dravins et al. (1981; Dravins 1982) have summarized the current understanding of the influence of solar granulation on spectral line asymmetries. The combination of the following three effects causes the typical line bisector shape to resemble the letter "C": Firstly, the combined effect of faster velocities and lower intensities from cold sinking convective elements, and slow velocities and higher intensities from hot rising elements depresses the red wing of the line near the continuum, which is responsible for the upper part of the "C" shape line bisector. Secondly, the net effect of a larger area of

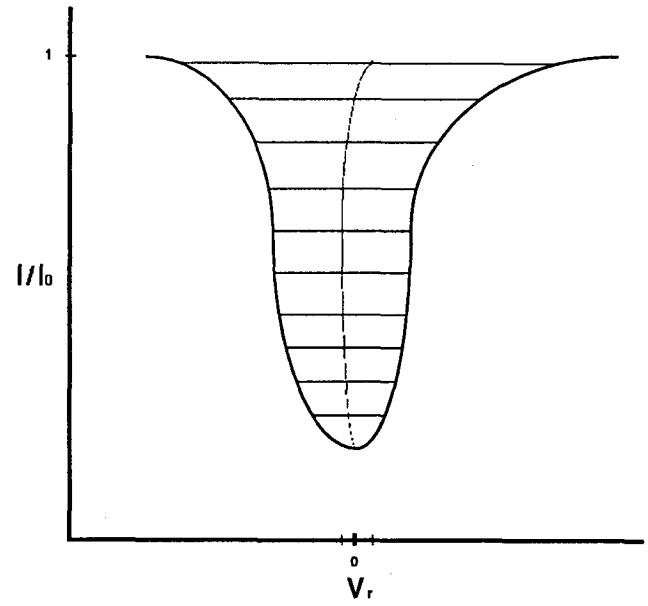

Fig. 1.— A line bisector, which is a locus of midpoints between the sides of the profile, is the observationally accessible gross parameter of stellar convection.

hot, rising convective elements and smaller regions of cool sinking elements is the depression of the blue wings of absorption lines. Therefore, the bisectors are generally convex towards the shortward wavelength side in the middle part of lines, which cause the middle part of the "C" shape. Finally, at the solar disk center, the core of a typical strong absorption line shows a smaller blue shift since it is formed higher in the atmosphere where the granulation motion does not reach. Thus, the bottom part of the typical line bisector resembles that of the "C" shape.

(c) The Granulation Boundary

More recent observations have found that spectral line asymmetries are also present in other stars. A systematic observation of the variations of stellar line bisectors was pioneered by Gray (1980, 1981). His extensive survey of the line bisectors of different luminosity classes and different spectral types stars showed that stars have systematically different line bisector shapes, and, therefore, different characteristics of stellar convection (Gray 1982, 1988; Gray and Nagel 1986). In the course of such studies, a 'granulation boundary' was proposed (Gray 1982; Gray and Nagel 1989).

The 'granulation boundary' distinguishes two regions in the HR diagram, such that the curvature of the line bisector is oppositely oriented on either side. In the cooler part of the HR diagram, the bisector is similar to the solar line bisector, which is shaped like a distorted letter "C", or like the top half of a "C" (a "C"-shape bisector, hereafter). Stars on the hotter side in the HR-diagram show bisectors of reversed curvature (a reversed "C"-shape bisector). Furthermore, the transition of the bisector curvature is continuous across the boundary on the HR diagram (Gray and Toner 1985; Gray and Nagel 1989). This granulation boundary, defined by Gray and Nagel (1989), runs from F0V to G1Ib stars.

To explain different bisector shapes on both sides of the granulation boundary, and to deduce the characteristics of stellar photospheric convection, only schematic models such as the two-stream model (Gray and Toner 1985, 1986), and the four-component model (Dravins 1990), have been employed. Using a two stream model of stellar granulation, which consists of a hot rising stream and a cold sinking one, Gray and Toner (1985) successfully reproduced the gradual bisector shape change among late-type stars by changing the average velocities of the two streams and the flux contrast between them. When the contribution from the cool stream is small or negligible, this model reproduces the reversed "C"-shaped bisector shape of hotter stars (Gray and Toner 1986). Dravins (1990) adopted another description of stellar granulation to understand the reversed "C"-shaped bisectors. At first, he has tried to incorporate the results of the hydrodynamic simulations, which Å. Nordlund *et al.* has computed (Dravins 1987ab ; Nordlund and Dravins 1990; Dravins and Nordlund 1990ab). This effort has been applied to a limited number of cases only. The opacity binning method and the anelastic approximation utilized for their numerical simulations, are responsible for the rather limited success. For more general studies, he devised the "four-component model" of convection.

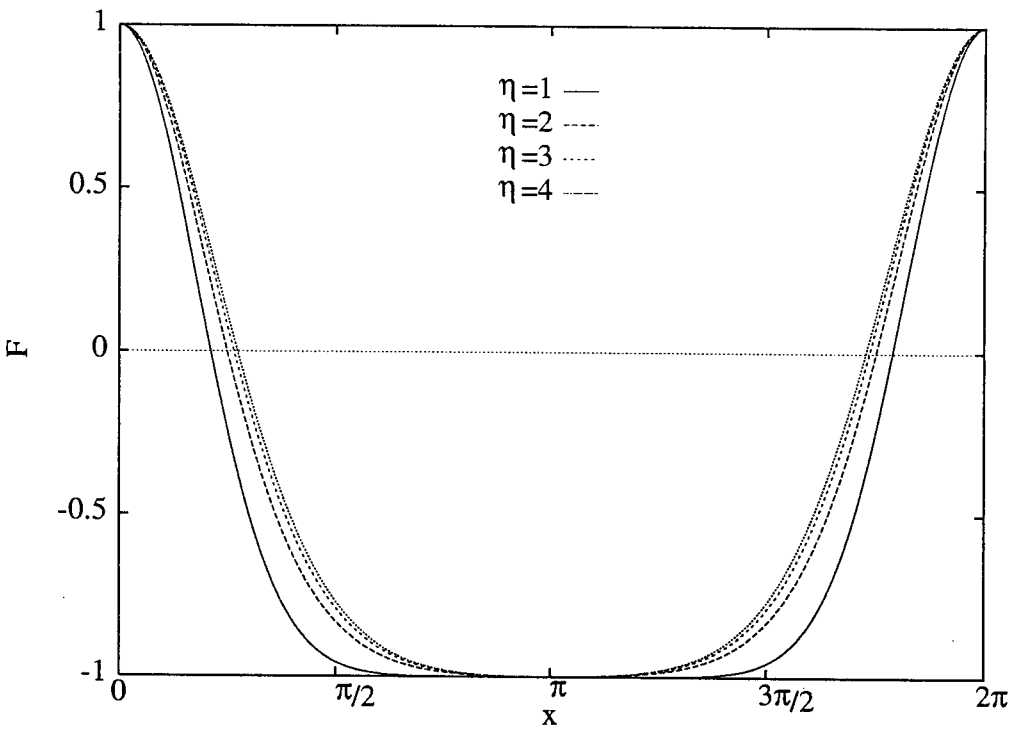

Fig. 2.— A simple granule model is prescribed with equation (1) through (3). The shape of the cosine function $F = \frac{1}{2\eta}[(\cos(x + \frac{\pi}{4}\sin x) + \eta)^2 - \eta^2 - 1]$ is shown here, which resembles the second term at the right hand side of equation (1) and (2). The shape of the function is controlled with a parameter η.

His four-component model consists of hot rising granules, cool sinking intergranular lanes, granular centers, and average-temperature stationary 'neutral regions'. The combination of contributions from these four components, weighted for their respective area coverage, brightness, line absorption, and Doppler shift, also reproduces the observed bisector shapes. The convection required for the reversed "C"-shaped bisector is characterized by concentrated, rapidly rising 'granules', surrounded by more extended regions of slower downfall.

(d) Motivation and Method

It is clear that the motion of gas on a stellar surface does not consist of a few independent flows. It is a continuous flow of fluid. Both the two-stream model (Gray and Toner 1985, 1986) and the four-component model (Dravins 1990) assumed that only a few discrete components of the motion of gas result in spectral line asymmetries. Furthermore, these components were chosen intuitively, with little justification. For example, horizontal flows were not considered in either model. Because the mean horizontal component of the velocity vectors should be zero, there should be no net asymmetry. This assumption is yet to be tested.

Therefore, we take a different approach. We have modelled the granule itself, rather than a few discrete flows. An analytical function is developed to depict the surface structure of solar granules. Based on the surface distribution of temperature and velocity vectors, a characteristic synthetic spectral line bisector is calculated. By deforming the analytical functions, we study the change of the characteristic bisector shapes as a function of surface feature type. Using this approach, we test the validity of those discrete component models.

Note that this simple granule model prescribes only the surface fluctuations of the temperature and the velocity fields. Calculating synthetic spectral lines using this granule model, therefore, is based on the assumption that the spectral lines are formed at a single surface. Even though real spectral lines are formed throughout stellar atmosphere, line forming regions are so thin that this assumption is reasonable for a crude calculation like this one. The two-stream model (Gray and Toner 1985, 1986) and the four-component model (Dravins 1990) also used the same assumption. Therefore, one must remember, with these simple models, that the lack of depth-dependent variation precludes the study of the effect of depth-dependent Doppler velocities on spectral line bisector.

II. A SIMPLE GRANULE MODEL

A set of simple analytical functions is designed, with which the observed characteristics of the Solar granules

Table 1. *Standard values of parameters for simple line synthesis*

Parameter	Value	Description
n	2800	Number of granule per radius
T_0	5770K	Temperature offset
ΔT	150K	Amplitude of Temperature fluctuations
V_{r0}	1.0 $km\ sec^{-1}$	Radial velocity offset
ΔV_r	2.0 $km\ sec^{-1}$	Amplitude of radial velocities
ΔV_h	1.5 $km\ sec^{-1}$	Amplitude of horizontal velocities
η	1	A controlling parameter of area coverage of flows
ϵ	1	A controlling parameter of area coverage of flows

can be described. This simple granule model depicts the surface fluctuation of temperature and the velocity field across a granule. The velocity fields and the temperature fluctuations at a horizontal location (θ, ϕ) on a stellar surface are prescribed as follows

$$T = T_0 - \frac{\epsilon \Delta T}{2\eta}[(\cos\hat{\theta} + \eta)(\cos\hat{\phi} + \eta) - \eta^2 - 1], \quad (1)$$

$$V_r = V_{r0} + \frac{\epsilon \Delta V_r}{2\eta}[(\cos\hat{\theta} + \eta)(\cos\hat{\phi} + \eta) - \eta^2 - 1], \quad (2)$$

$$V_h = -\Delta V_h \sin\hat{\theta} \sin\hat{\phi}, \quad (3)$$

where

$$\hat{\theta} = n\theta + \frac{\pi}{4}\sin(n\theta), \qquad \hat{\phi} = n\phi + \frac{\pi}{4}\sin(n\phi),$$

T_0 is the temperature offset, ΔT is the temperature fluctuation, V_{r0} is the offset of the radial velocities, ΔV_r is the radial velocity fluctuation, and ΔV_h is the horizontal velocity fluctuation. The parameter η, which is an integer bigger than 1, and ϵ, which is $+1$ or -1, are the controlling parameters for the surface area coverage of up- and down-flows. η changes the shape of the fluctuations. The shape of the function in the second term of the right hand side for different values of η are shown in figure 2. The parameter ϵ inverts the function. Downflows are defined to have positive V_r.

A cross-section of one model granule is shown in figure 3. This simple description of granulation was designed to have the observed characteristics of solar granulation. For example, the mean radial velocity is not zero when the area coverage of up- and down-flow is equal. The temperature fluctuations and the radial velocities are correlated, while both are anti-correlated with the horizontal velocities. Those hot and rising convective flows cover more area than do the cold and sinking flows. The speed of sinking elements is faster than that of rising ones. By changing the controlling parameters, (T_0, ΔT, V_{r0}, ΔV_r, ΔV_h, η, and ϵ), this simple function can model different convective activities, which may arise under other stellar photospheric conditions.

III. LINE SYNTHESIS

To a first approximation, the inverted full-disk Doppler-shift distribution can be used for the study of the effect of this model granulation on spectral lines. This approximation holds in the linear part of the curve of growth, where line strength is proportional to the number of absorbing particles. Since we are interested in the *qualitative* effect on line *asymmetries*, and since the thermal broadening is *symmetric*, this can be a good first approximation.

When the velocities of granulation are larger than the thermal motions, the detailed thermal profiles are not so important for this crude calculations. The model granules, i.e. the velocity fields and the temperature fluctuation, are distributed on the surface of a sphere. The total number of granules is controlled by n in the above equations. The temperatures and velocities on the sphere are sampled at 900 × 3600 locations. At each location (θ, ϕ), the thermal velocity dispersion is calculated: ${\sigma_r}^2 = {\sigma_t}^2 = \frac{2kT}{m}$, where σ_r and σ_t are the dispersions of the radial and the tangential velocity distribution respectively(for simplicity, we assume $\sigma_r = \sigma_t$ in this paper), k is the Boltzmann constant, T is the local temperature, and m is the mass of the elements for the spectral line we are studying (m = 55.847 for Fe). The total velocity dispersion is

$$\sigma^2 = {\sigma_r}^2 \cos^2\theta + {\sigma_t}^2 \sin^2\theta.$$

The intensity from a location where the temperature is T is assumed to be

$$I_0 = \frac{2hc/\lambda^3}{\exp\frac{hc}{k\lambda T} - 1},$$

where h is the Planck constant, c is the speed of light, and λ is the wavelength of the line under scrutiny. λ = 5000Å is used. Taking into account the limb darkening, the intensity from a horizontal location (θ, ϕ) becomes

$$I = I_0(1 - \varepsilon + \varepsilon\cos\theta),$$

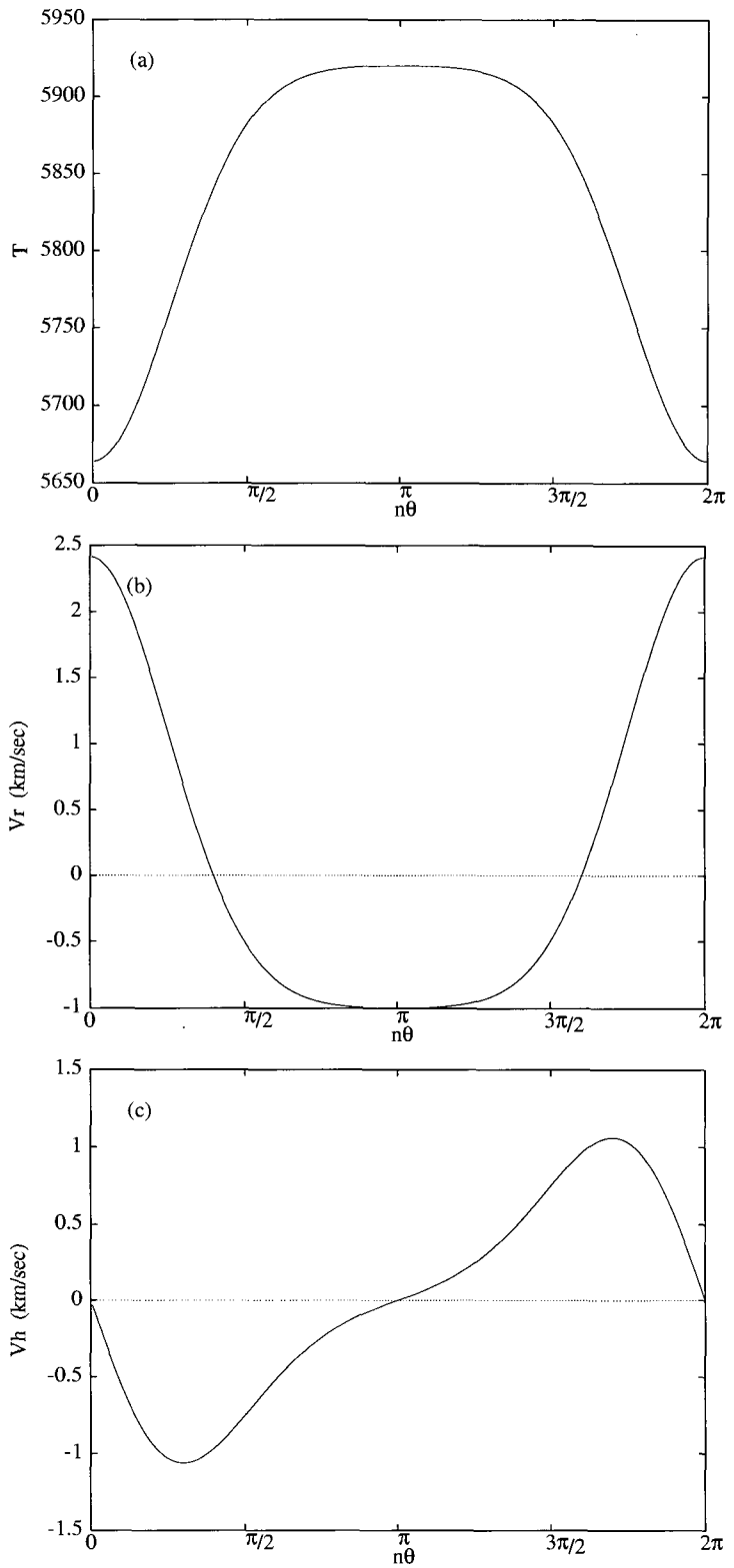

Fig. 3.— A cross section of a model granule with $\epsilon = \eta = 1$, $\hat{\phi} = \frac{\pi}{4}$, $T_0 = 5770K$, $\Delta T = 150K$, $V_{r0} = 1.0km/sec$, $\Delta V_r = 2.0km/sec$, and $\Delta V_h = 1.5km/sec$. The temperature (a), vertical (b), and horizontal (c) velocity distribution are shown across a diameter of a model granule.

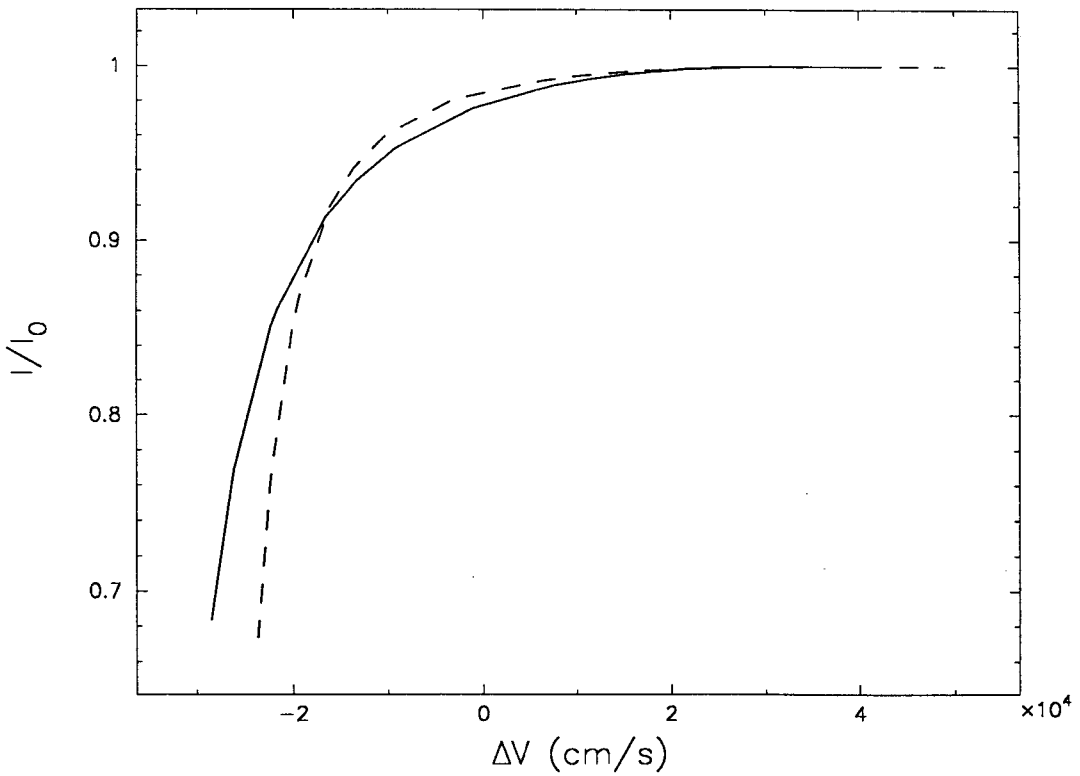

Fig. 4.— Effect of horizontal flows on line bisectors. The solid line shows the bisector calculated with the standard values in table 1. The dashed line shows the bisector calculated with the standard values, except $\Delta V_h = 0$.

where ε is the limb darkening parameter, $\varepsilon = 0.54$ is used (Allen 1976). Then, assuming the Gaussian distribution of velocities V, the Doppler distribution weighted with the intensity and the surface area is:

$$P(V) = \sum_{\theta=0,90,\phi=0,360} \frac{I}{2\pi\sqrt{\pi}\sigma} \exp \frac{-(V - V_D)^2}{\sigma^2} \cdot \times \sin\theta \cos\theta \Delta\theta \Delta\phi,$$

where V_D is the Doppler velocity which is the projection of the velocity vectors at each location to the line of sight. The calculation of the Doppler velocities is discussed in the Appendix. Therefore, the line profile can be approximated as $1 - CP(V)$, where C is a scaling factor.

Using the values shown in table 1, which resemble those of solar granulation, the procedure described above was used to calculate a synthetic Fe line at $\lambda = 5000$Å, and its bisector. For the standard parameters, 70 percent of the area is covered by upflows. The maximum downward velocity is 3.0 $km\ sec^{-1}$, and the maximum upward velocity is 1.0 $km\ sec^{-1}$.

IV. THE EFFECT OF CONVECTION ON A SYNTHETIC SPECTRAL LINE

To study the effect of each parameter on the line bisector shape, several line bisectors were calculated using different parameters.

(a) The Effect of Horizontal Flows

Figure 4 shows the effect of horizontal flows. The solid line shows the bisector which is calculated using the standard values, whereas the dashed line shows the bisector calculated using the standard values except $\Delta V_h = 0$. When the contribution of horizontal velocities is ignored, the amplitude of the Doppler velocity distribution is reduced. Therefore, the curvature of the line asymmetry is reduced accordingly. It is clear that, while the general sense of asymmetry is preserved, the effect on the amplitude of the line asymmetry is non-negligible when the horizontal velocities are comparable to the vertical velocities. Note that the effects of horizontal flows were not included in the two-stream model (Gray and Toner 1985, 1986) or in the four-component model (Dravins 1990).

(b) The Effect of the Number of Granules

While keeping all the other values constant, the number of granules was varied. Whether n was 2800, 700, or 50, no noticeable change was found in the area coverage, and therefore in the line bisector shape. Only for $n = 5$ was the area coverage of upflows reduced, from the usual 70 percent to 66 percent, causing a line shift while preserving the bisector shape.

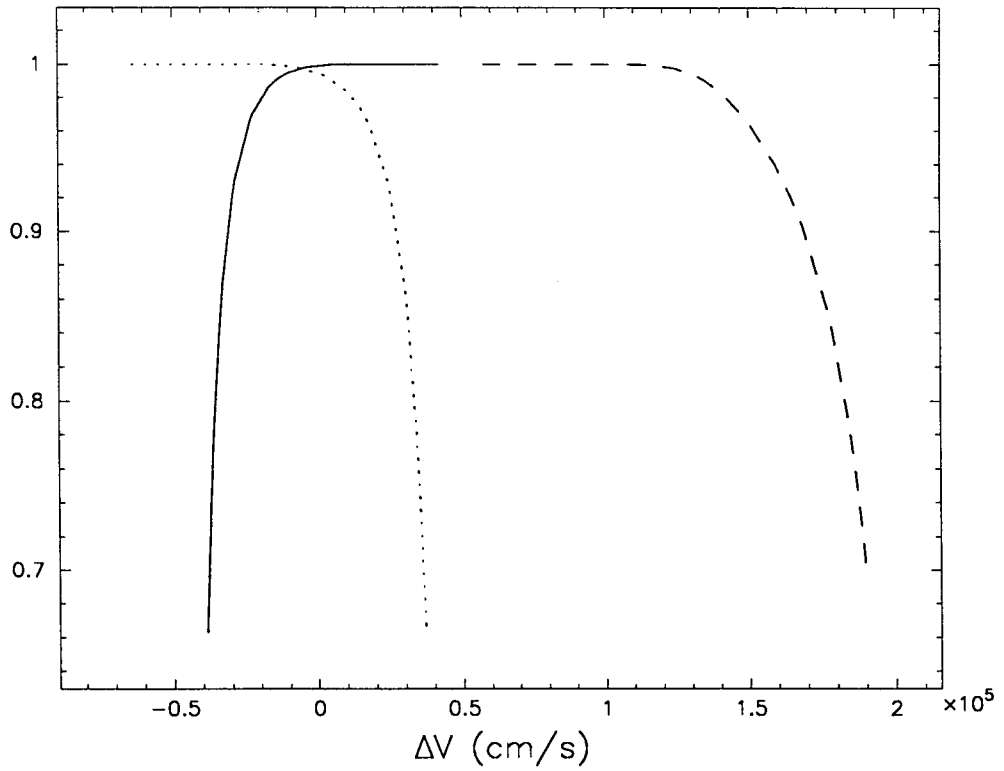

Fig. 5.— Effect of area coverage of flows on line bisectors. The solid line shows the bisector calculated with the standard values in table 1 except $n = 5$. The dashed line shows the bisector calculated with the standard values, except $n = 5$, $\epsilon = -1$. The dotted line shows the bisector calculated with the standard values, except $n = 5$, $\epsilon = -1$, $V_{r0} = -1.0\ km\ sec^{-1}$, and $\Delta V_r = 2.0\ km\ sec^{-1}$.

(c) The Effect of the Area Coverage

By changing ϵ, the area coverage is inverted. When $\epsilon = -1$, the model convection has 95 percent of area covered by down flows, the maximum upward velocity is 1 $km\ sec^{-1}$, and the maximum downward velocity is 3 $km\ sec^{-1}$. The bisector, the dashed line in figure 5, is not only red shifted, but also the "C" shape is reversed. V_{r0} and ΔV_r are adjusted so that the model convection is the exact opposite to the standard case (with $n = 5$), i.e. the model has 66 percent of the surface area covered by down flows, the maximum downward velocity is 1 $km\ sec^{-1}$, and the maximum upward velocity is 3 $km\ sec^{-1}$. The reversed "C"-shaped line bisector is shown as the dotted line.

(d) The Effect of the Temperature Fluctuation

For the three cases shown in figure 6, the amplitude of the temperature fluctuation, ΔT, was varied. The line bisectors for $\Delta T = 150$, 1500, 4000 are shown as the solid line, the dashed line, and the dotted line, respectively. The temperature contrasts correspond, respectively, to the intensity contrasts $\Delta I/I_0 = 0.24$, 3.66, and 14.14. As the relative contribution of downward flows gets smaller, the bisector shapes change from "C" shape to reversed-"C" shape. When the intensity contrast is large, observers can 'see' only rising flows ("Expanding star effect" Gray 1988). The weighted Doppler distribution will have enhanced blue wings. Therefore, the synthetic spectral line will have the reversed-"C" shape.

(e) The Effect of Rotation

The effect of rotation is shown in figure 7. When a rotational velocity of 1.5 $km\ sec^{-1}$ at equator is introduced, the curvature of the line bisector is changed so that the bottom of the bisector shifts blueward. This effect arises because the rotation alters the Doppler distribution. As the effects of rotation are maximum at the limb of a star, it effectively pushes the wing of the distribution curve outward from line center. Since the rotation does not affect the disk center, the Doppler distribution is deformed so that the top part of the distribution, i.e. the bottom part of the line bisector is blue shifted.

V. SUMMARY AND DISCUSSION

A simple line synthesis using a simple 'model' of granulation was conducted. The intensity contrast, and the relative area coverage of up- and down-flows are the two main factors which determine the spectral line bisector shape. This justifies the assumption of the aforementioned discrete-flow models (Gray and Toner 1985,

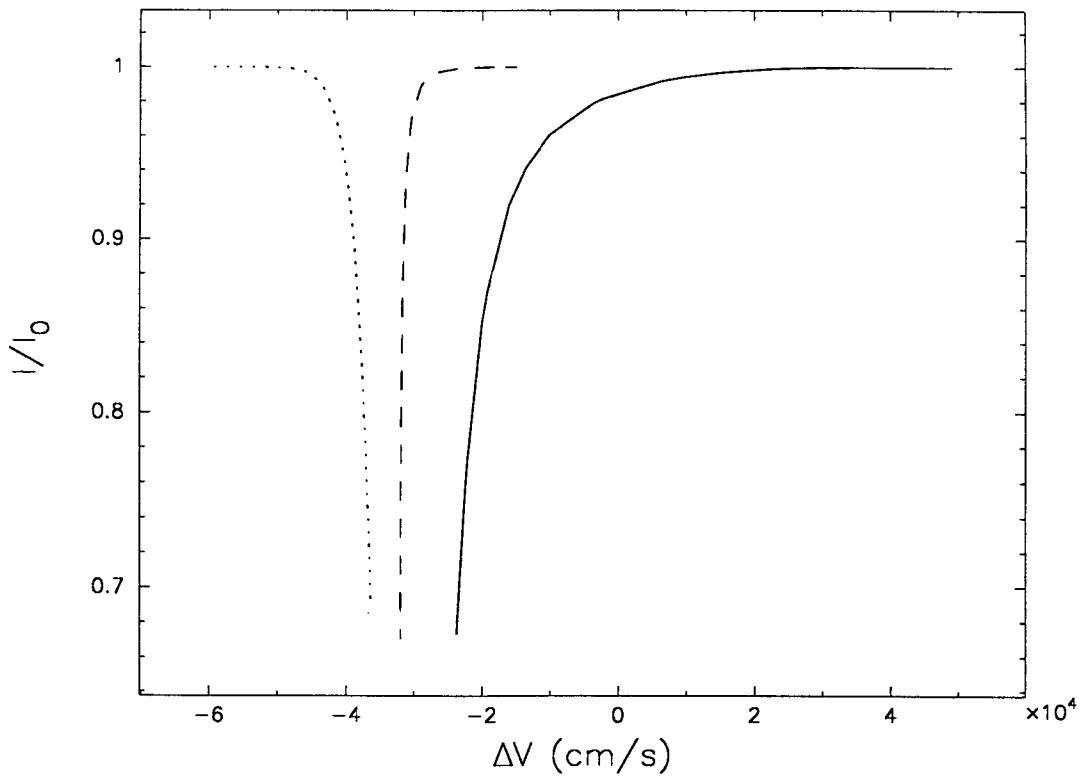

Fig. 6.— Effect of temperature fluctuation on line bisectors. The solid line is for $\Delta T = 150K$, the dashed line is for $\Delta T = 1500K$, the dotted line is for $\Delta T = 4000K$. All the other parameters are the same for all three cases.

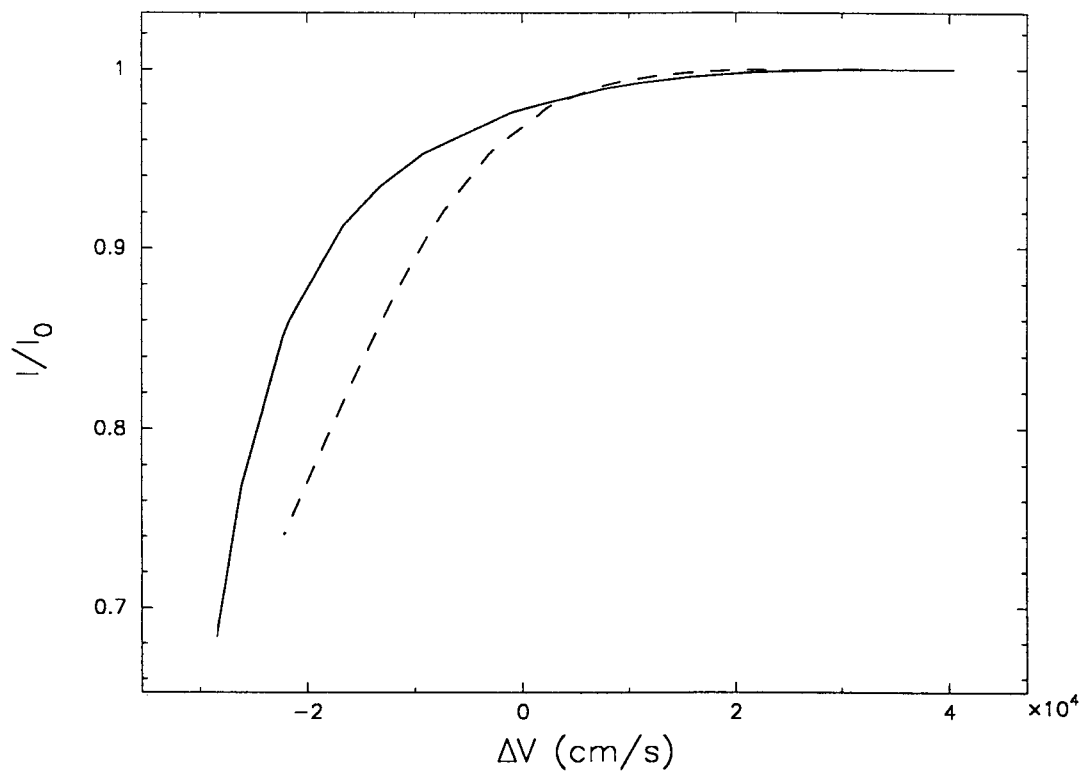

Fig. 7.— Effect of rotation on line bisecotrs. The solid line is from the standard calculation. The dashed line is from the case where a rotational velocity 1.5 $km\ sec^{-1}$ is included.

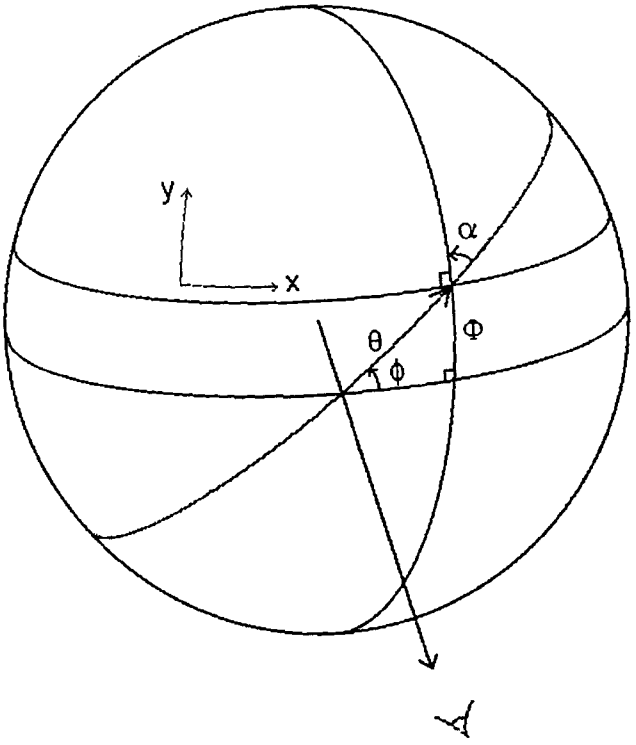

Fig. 8.— Three angles are defined for disk integration. θ is the limb distance. ϕ is the angle between the plane normal to the projected rotational axis and the plane containing the visual disk center, the center of the sphere, and a location on the surface at which one wants to know the rotational velocity component. To describe the relation between the two angles, two more angles, α and Φ, are defined as shown on the plot. From simple spherical trigonometry, we obtain the following relation between angles: $\sin\Phi = \sin\theta \sin\phi$, $\cos\alpha = \sin\phi \cos\theta / \cos\Phi$.

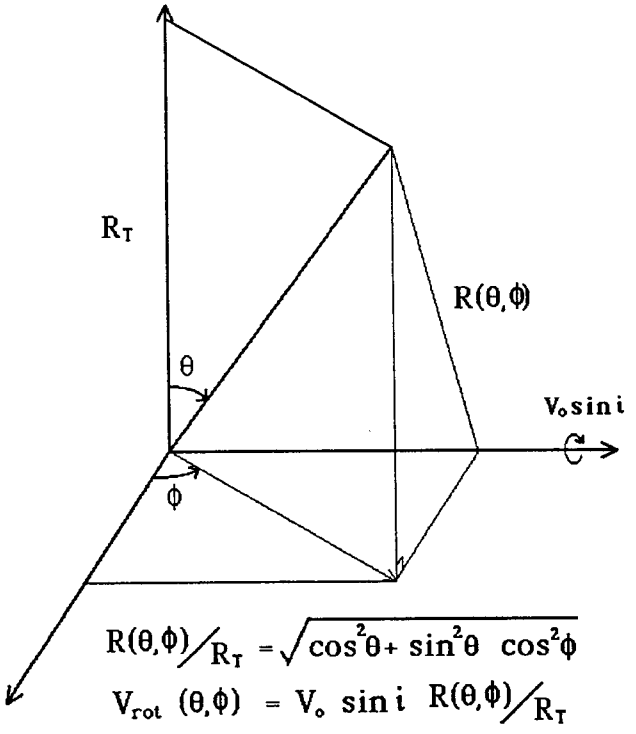

Fig. 9.— Projected rotational velocity on the surface of a star as a function of the location.

1986; Dravins 1990).

While the vertical flows are the important ones in shaping the spectral line asymmetries, the horizontal flows are not negligible in shaping the curvature of the line bisectors. As a convective element moves up (or down) it expands (contracts). This expansion (contraction) is one component of horizontal flow. These horizontal flows affect the Doppler velocity distribution as rotation does. Therefore, much care must be taken to distinguish the effect of rotation from that of horizontal flows. Since horizontal flows affect line bisector shaping as well as line broadening, more simple models with only vertical flows taken into account (Gray and Toner 1985, 1986; Dravins 1990), produce less reliable information of the effect of convection on spectral line asymmetries.

From this exercise using a simple model of granules, we were able to obtain the characteristic "C" shaped bisector when we used the adjustable parameters in the model for the Sun. The reversed-"C" shaped bisector can be obtained when the flow pattern is opposite to that of the Sun, i.e. downflow dominant convection, or when the temperature fluctuation is much larger than that of the Sun. Even when hot upflows cover more regions (as in solar granulation), the temperature contrast is so large that spectral lines formed throughout the sinking region is negligible, resulting in a reversed-"C" shape. These results are based on the assumption that the velocity fields and temperature fluctuations are positively correlated. Therefore, there is another possible way to obtain the reversed-"C" shaped bisector. When upflows are cold and downflows are hot, the convection causes spectral lines to be reversed-"C" shaped. (*cf.* Gray and Toner 1985, 1986; Dravins 1990; De Jager 1990)

This exercise, described in this paper, provides a qualitative understanding of the effect of convection on spectral lines. This knowledge can be served as a guide line for the detailed line synthesis calculated using the hydrodynamic convection simulations (*cf.* Kim and Fox 1992; Kim 1993).

ACKNOWLEDGEMENTS

I am indebted to Dr. Gray for his guidance on calculations of disk integrated synthetic lines. In addition, his two-stream model inspired me to develop the simple granule model presented in this paper. I would like to thank P. A. Fox and P. Demarque for their constructive comments. This research has been supported in part by the Creative Research Initiative Program of Korean Minitry of Science and Technology, to the Center for Space Astrophysics Yonsei University. Additional support has been provided in part by NASA grant NAG5-2795 to Yale University.

REFERENCES

Allen, C. W. 1976, Astrophysical Quantities, 3rd ed., (London: Athlone)

De Jager, C. 1990, Solar Phys., 126, 201

De Jager, C. and Neven, L. 1967, Solar Phys., 1, 27

Dravins, D. 1982, ARA&A, 20, 61

Dravins, D. 1987a, A&A, 172, 200

Dravins, D. 1987b, A&A, 172, 211

Dravins, D. 1990, A&A, 228, 218

Dravins, D., Lindegren, L., and Nordlund, Å. 1981, A&A, 96, 345

Dravins, D. and Nordlund, Å. 1990a, A&A, 228, 184

Dravins, D. and Nordlund, Å. 1990b, A&A, 228, 203

Gray, D. F. 1980, ApJ, 235, 508

Gray, D. F. 1981, ApJ, 251, 583

Gray, D. F. 1982, ApJ, 255, 200

Gray, D. F. 1988, Lectures on Spectral-Line Analysis: F, G, and K Stars, (Arva, Ontario:The Publisher)

Gray, D. F. and Nagel, T. 1989, ApJ, 341, 421

Gray, D. F. and Toner, C. G. 1985, PASP, 97, 543

Gray, D. F. and Toner, C. G. 1986, PASP, 98, 499

Gurtovenko, E. A. 1972, Astrom. Astrofiz., 16, 77

Gurtovenko, E. A., Kostik, R. I., Orlova, T. V., Troyan, V. I., and Fedorchenko, G. L. 1975, Profili izbrannyh fraungoferovyh linij dlja raznyh polozhenij tsentr-kraj na diske Solntsa, (Kiev: Naukova Dumka)

Halm, J. 1907, Astron. Nachr., 173, 273

Higgs, L. A. 1960, MNRAS, 121, 421

Higgs, L. A. 1962, MNRAS, 124, 51

Jewell, L. E. 1896, ApJ, 3, 89

Kim, Y. -C. 1993, Ph. D. Thesis, Yale University

Kim, Y. -C. and Fox, P. A. 1992, in Cool stars, stellar systems, and the Sun, eds. M. S. Giampapa and J. A. Bookbinder, p 172

Kostik, R. I. and Orlova, T. V. 1970, Astrom. Astrofiz., 9, 117

Kostik, R. I. and Orlova, T. V. 1977a, Astrom. Astrofiz., 33, 51

Kostik, R. I. and Orlova, T. V. 1977b, Solar Phys., 53, 353

Magnan, C. and Pecker, J. C. 1974, Highlights of Astr., 3, 171

Melnikov, O. A. 1964, Izv. Glav. Astron. Obs. Pulkovo, 23, 3

Nordlund, Å. and Dravins, D. 1990, A&A, 228, 155

Pierce, A. K. and Breckinridge, J. B. 1973, Kitt Peak Nat. Obs. Contr., 559

Voigt, H. H. 1956, ZAp, 40, 151

Voigt, H. H. 1957, ZAp, 47, 144

APPENDIX

When the angles, α, θ, ϕ are defined as shown in the figure 8, the Doppler velocities along a line of sight,V_D, are calculated from the projection of the velocity component (V_x, V_y, V_z) at each depth point.

$$\alpha = \cos^{-1}\left(\frac{\sin\phi\cos\theta}{\sqrt{1-\sin^2\theta\sin^2\phi}}\right), \tag{1}$$

$$V_{rot}(\theta,\phi) = V_0 \sin i \sqrt{\cos^2\theta + \sin^2\theta\cos^2\phi}, \tag{2}$$

$$V_h = \begin{cases} V_y\cos\alpha - (V_{rot}+V_x)\sin\alpha, & \text{if } \frac{\pi}{2} \le \phi \le \frac{3\pi}{2}\ ; \\ V_y\cos\alpha + (V_{rot}+V_x)\sin\alpha, & \text{otherwise.} \end{cases} \tag{3}$$

$$V_D = -V_z\cos\theta + V_h\sin\theta \tag{4}$$

where V_0 is the rotational velocity at the equator, i is the angle between the rotational axis and the line of sight, and V_{rot} (in figure 9) is the rotation velocity at the horizontal location at the surface. The minus sign in the right hand side of equation (4) is introduced to correct the sign so that the upflows cause blue-shift in the synthetic spectral line. The above equations are derived considering a general case. For the line synthesis in this paper, $V_x = V_y = V_h$ and $V_z = -V_r$.